Journal of The Electrochemical Society, **155** (10) 1-XXXX (2008)
0013-4651/2008/155(10)/1/0/$23.00 © The Electrochemical Society

Electrochemical Methods to Enhance the Capacitance in Activated Carbon/Polyaniline Composites

María J. Bleda-Martínez,[a] Chuang Peng,[b] Shenguen Zhang,[b] George Z. Chen,[b,*] Emilia Morallón,[a,*,z] and Diego Cazorla-Amorós[c]

[a]*Departamento de Química Inorgánica., Universidad de Alicante., E-03080, Alicante, Spain*
[b]*School of Chemical and Environmental Engineering, University of Nottingham, University Park, NG7 2RD Nottingham, United Kingdom*
[c]*Departamento de Química-Física and Instituto Universitario de Materiales, Universidad de Alicante, E-03080, Alicante, Spain*

Activated carbon/polyaniline composites have been prepared using different electrochemical methods: single-step potentiostatic polymerization, multiple-step potentiostatic polymerization, and potentiodynamic polymerization with the anodic potential limits being fixed at either 0.75 or 1 V (vs Ag/AgCl). The prepared composite samples were characterized by cyclic voltammetry, galvanostatic charge-discharge tests, electrochemical impedance spectroscopy, and Fourier transform infrared (FTIR) spectroscopy. The synthesis conditions were found to strongly affect the electrochemical behavior of the samples. High capacitance was achieved by the potentiostatic polymerization methods. As a general trend, higher capacitance and lower resistance were observed in the composites than the sum of these parameters of the individual components. This benefit is attributed to the enhanced electron delocalization along the polymer chains in the composites resulting from the influence of the activated carbon, as evidenced by the FTIR. However, an influence of the polyaniline morphology induced by the porous carbon cannot be discarded.
 [DOI: 10.1149/1.2956969]

AQ: #1

Manuscript submitted January 9, 2008; revised manuscript received June 18, 2008.

In recent years, fast-growing concerns over the anticipated fossil fuel exhaustion and the negative impact of their use on the environment have become the strong driving force for the development of processes and devices that can help with more efficient utilization of energy. Particularly, electrochemical capacitors or supercapacitors have received special attention because of their high-power capability and long cycle life. The electrode materials commonly used in supercapacitors include porous carbons, conducting polymers, and some transition metal oxides.[1,2] Hydrous ruthenium oxides are thus far the champion in specific capacitance,[3-6] but they are too expensive to be commercially used on a large scale. Alternatively, porous carbons, conducting polymers, and, as an example, manganese oxides have been demonstrated in the literature to be more affordable and environmentally friendly.[2]

Porous carbons have been widely studied as supercapacitor electrode materials. Previous research has shown that the porosity is the main factor affecting the double-layer contribution to capacitance.[1,7] In such cases, the porosity development in porous carbons has a limit as does the capacitance. Recently, additional faradaic contributions or pseudocapacitance from the surface functional groups in the porous carbons have been identified.[8-12] Thus, the capacitance of porous carbons may be further enhanced by taking advantage of the pseudocapacitance (redox contribution) from the chemical species bonded or added to the carbon material.

Conducting polymers are typical examples of pseudocapacitance performance because they can offer a continuous range of oxidation states by increasing the electrode potential.[1] Of all investigated conducting polymers, polyaniline is perhaps the easiest and cheapest to synthesize chemically or electrochemically in aqueous media. Also, doped polyaniline is much more conductive in comparison to the other common conducting polymers. It is extremely stable in either dry or wet air but can undergo kinetically fast doping/dedoping switching.[13-16] When made into thin films, polyaniline can offer a specific capacitance value in the range of 700–800 F/g[16-18] but thicker films were often found to be inferior in performance.[18] It is also known that the redox behavior of polyaniline depends largely on morphology and structure that affect the specific surface area and the ion diffusivity.[18-20] Taking into account these facts, deposition of polyaniline as a thin film dispersed over a support with prescribed high surface area and pore structure seems to be an effective approach toward improved electrochemical capacitance. In fact, a few successful attempts have already been carried out on carbon materials as the support for polyaniline.[15,21-29] In these studies, remarkable cooperative effects between the carbon material and the polymer were observed. It was thought that the former provided better mechanical properties[22] and high surface area, whereas the latter could grow as thin films to allow better redox kinetics.[15]

However, to our knowledge, there is not yet a systematic study of the influence of the electrochemical preparation method on the properties of the carbon/polyaniline composites. In this work, polyaniline was electrodeposited onto a high-surface-area activated carbon by different methods, namely, single-step potentiostatic polymerization, multistep potentiostatic polymerization, and potentiodynamic polymerization. In addition, two different oxidation potentials for the polymerization were applied. The advantages and disadvantages of each method have been compared and discussed.

Experimental

Preparation and characterization of the activated carbon.— Anthracite was chemically activated using KOH as the activating agent. The activating agent/carbon ratio employed was 3:1. The activation was achieved by heating the mixture at 750°C for 1 h under nitrogen flow rate of 800 mL/min. Details of the activation process are available elsewhere.[30] The porous texture of the sample was determined by physical adsorption (N_2 at 77 K and CO_2 at 273 K) using an automatic adsorption system (Autosorb-6, Quantrachrome) after sample outgassing at 523 K under vacuum for 4 h. The total volume of micropores (pore size of <2 nm) was calculated by the application of the Dubinin–Radushkevich (DR) equation to the N_2 adsorption at 77 K. The volume of narrow micropores (pore size of <0.7 nm) was assessed from CO_2 adsorption at 273 K using the DR equation.[31] The densities of the adsorbed phase used for the calculations were 0.808 and 1.023 g/mL for N_2 and CO_2,[31] respectively. The apparent surface area was calculated by the Brunauer, Emmett, and Teller (BET) equation.

Electrochemical system.— All electrochemical measurements were carried out on a potentiostat/galvanostat (Autolab model PGSTAT30 or EG&G model 273 controlled by software ECHEM M270). A standard three-electrode cell was used to accommodate the electrochemical tests with an Ag/AgCl reference electrode and a graphite bar as a counter electrode. An aqueous solution of

AQ: #2

* Electrochemical Society Active Member.
z E-mail: morallon@ua.es

Table I. Carbon/polyaniline composite samples and the electrosynthesis methods.

Samples	Type	Method	Potential range (V)
A	Activated carbon	—	—
AP1	Composite	Single potential step	0.30–1.0
AP75	Composite	Single potential step	0.30–0.75
AD1	Composite	Potentiodynamic	0–1.0
AD75	Composite	Potentiodynamic	0–0.75
AS1	Composite	Multiple potential step	0.30–1.0
AS75	Composite	Multiple potential step	0.30–0.75

1.0 M HCl + 0.5 M KCL prepared with Merck p.a. chemicals, was used as the electrolyte in all electrochemical synthesis and analysis experiments.

Electrodes fabrication.— A paste of the porous activated carbon mixed with a binder (PTFE) (20 wt %) was spread and pressed uniformly and thinly with a spatula onto a graphite disk electrode (0.6 cm diam). No conductivity promoter, such as acetylene black was used. After drying, the electrode was placed as the working electrode in a solution of 0.15 M aniline + 1.0 M HCl + 0.5 M MCl (Merck p.a. chemicals), and subjected to electropolymerization. Three methods were used, including (*i*) single potential step from the lower potential of 0.3 V (where no electrode reaction occurred) to an upper potential (where the polyimerization took place) of either 0.75 or 1.0 V for a time until the total charge passed was 2.0 C, (*ii*) potentiodynamic polymerization by cycling at 75 mV/s from 0 to either 0.75 or 1.0 V for 30 cycles, and (*iii*) multiple potential steps from the lower potential of 0.30 V to the upper potential (0.75 or 1.0 V) for 200 pulses with the pulse width being fixed at 4 s. For comparison, these electropolymerization methods were also used to grow polyaniline films on the graphite electrode under the same experimental conditions. For the convenience of discussion, Table I summarizes these different polymerization experiments and the names of the obtained samples.

The mass of the carbon material in all samples was ~1 mg. The total weight, carbon plus polyaniline, ranged from about 1.5–2.5 mg, depending on the polymerization method. Samples were weighed on a microbalance with an accuracy of ±1 μg (Sartorius Supermicro model S4).

Electrochemical characterization.— The galvanostatic charging/discharging method (at 0.5, 1.0, and 5.0 mA) was used to measure the capacitance. The geometric area of the electrodes was 28.3 cm^2. The capacitance values were calculated from the discharge time for the electrode potential to decrease from 0.6 to 0 V and are expressed in F/g taking into account the mass of both carbon and polyaniline in composite (but not the binder). The coulombic efficiency was also calculated. Cyclic voltammograms were obtained in order to assess the redox behavior of the samples. The applied scan rates were 1 and 10 mV s^{-1}. Electrochemical impedance spectroscopy was applied on these samples in order to study their resistive behavior. These analyses were carried out on a FRD-100 frequency response detector module connected to the EG&G model 273 potentionstat/galvanostat.

Infrared spectroscopy characterization.— The pristine activated carbon material, the activated carbon/polyaniline composites, and polyaniline films were analyzed by Fourier transform infrared (FTIR) spectroscopy. A Nicolet Continuμm FTIR microscope attached to a Nicolet 5700 FTIR spectrometer, equipped with a liquid nitrogen-cooled mercury-cadmium-telluride detector, was used. The spectra were acquired in the attenuated total reflection (ATR) mode using a Germanium crystal. The resolution employed was 16 cm^{-1}. Additional FTIR spectra were collected in the transmission mode.

Table II. Porous texture characterization of the pristine carbon material.

Sample	BET (m^2/g)	$V_{DR}N_2$ (cm^3/g)	$V_{DR}CO_2$ (cm^3/g)
A	2584	1.20	0.55

Results and Discussion

Porous texture characterization of the carbon material.— The pristine carbon material presented a type I isotherm for N_2 adsorption (not shown) as expected for microporous solids. Table II presents the BET surface area and the micropore volumes calculated from the N_2 adsorption data at 77 K [$V_{DR}(N_2)$] and CO_2 adsorption data at 273 K [$V_{DR}(CO_2)$] for the carbon sample.

Polymerization processes.— Electrochemical behavior of the carbon material in presence of aniline.— Figure 1 shows the voltammograms obtained for the activated carbon material in the absence and the presence of aniline in the 1.0 M HCl + 0.5 M KCl KCl solution. It can be observed that the activated carbon does not show any remarkable redox processes at these conditions. When the aniline is present in the solution, an oxidation current appears at 0.75 V. The cycling between 0 and 1.0 V produces an increase in the current in the whole range of potentials and the appearance of redox processes corresponding to the polyaniline formed during the cycling.

Single-step potentiostatic polymerization.— The chronoamperometric curves recorded after stepping the potential from 0.3 to either 0.75 or 1.0 V (figures not shown) are both featured by an exponential decrease of current in the initial period, which was followed by an increase. The first stage is usually related to the double-layer charging and the nucleation process. The subsequent increase of current is attributed to the linear growth of polymer chains.[32] The polymerization at 0.75 V is slower than at 1.0 V as judged by the recorded currents. Also, the increase of the current after the exponential decay was more pronounced in the polymerization at 0.75 V rather than at 1.0 V. In addition to the effect of an increased electrode surface area upon polymer deposition, it has been reported that this increase in current is related to the one-dimensional chain growth by means of direct monomer incorporation into the existing polyaniline film.[32] This mechanism is favored when the potential is not too high. It is also worth pointing out that the polymerization shows a higher current on the activated carbon electrode than directly on the bare graphite electrode, for both potentials. This can be a consequence of the much larger surface area of the activated carbon.

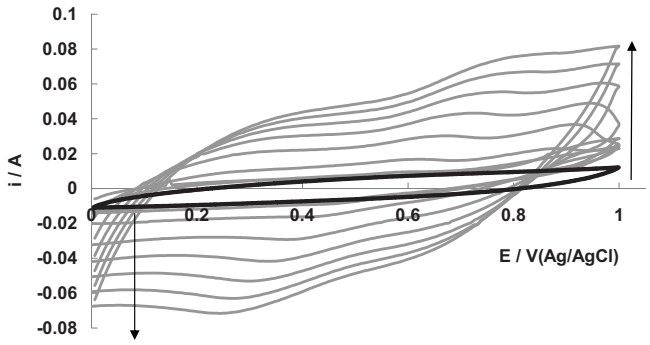

Figure 1. Steady cyclic voltammogram for the activated carbon in 1 M HCl + 0.5 M KCl solution (black line). Consecutive cyclic voltammograms in the presence of 0.15 M of aniline (gray lines). The arrow indicates the increase of the number of cycles from 1 to 30. The cycles presented are 1, 2, 5, 10, 15, 20, 25, and 30.

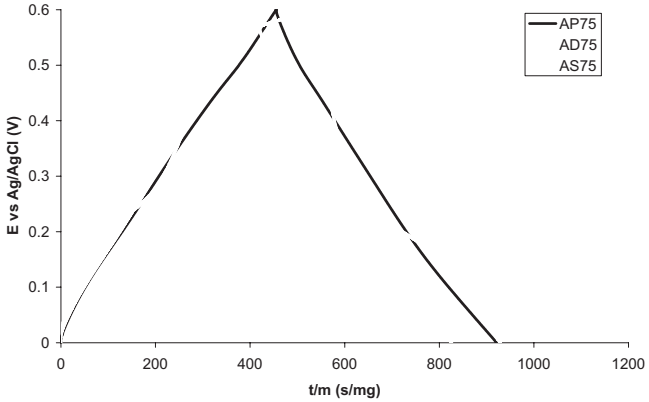

Figure 2. Charge–discharge cycles at 0.5 mA. 1 M HCl + 0.5 M KCl solution. Polymerization methods at 0.75 V.

Potentiodynamic polymerization.— In the potentiodynamic polymerization by cycling at 75 mV/s, a higher polymerization rate is obtained when the upper potential is 1.0 V, apparently due to more aniline molecules being oxidized and incorporated into the polymer chain. As in the single-step potentiostatic polymerization, the current was larger on the porous activated carbon electrode than that on the bare graphite electrode.

Multistep potentiostatic polymerization.— In this method, polymerization was achieved by the application of 200 alternative potentiostatic pulses from the lower potential of 0.30 V to the upper potential of 0.75 or 1.0 V. Each of the lower and upper potentials was maintained for 4 s. The current vs time was registered. When the pulses were carried out between 0.30 and 1.0 V, the amount of deposited polyaniline was larger, as expected.

Characterization by chronopotentiometry.— The activated carbon/polyaniline composites prepared in the above-described experiments were first characterized by chronopotentiometry. The samples were subjected to charge–discharge cycles by constant current of 0.5, 1.0, and 5.0 mA. The results for the experiments at 0.5 mA are plotted in Fig. 2 and 3. The *x*-axis (time) has been divided by the weight of the sample (~2 mg for all composites) so that the graphics can be directly compared. (Note that the time is proportional to the charge in these constant current experiments). All samples, except for sample AD75, exhibit a quasi-linear behavior in the whole potential range. The deviation for sample AD75 may be explained if the polymerization was incomplete during the preparation of the composites. Then, aniline and some oligomers could contribute to further polymerization during the characterization experiment producing a plateau at ~0.55 V in the chronopotentiogram. The capacitance of all the samples was determined from the discharge process. The coulombic efficiency was calculated from the charges in both charging and discharging processes. In general, this efficiency was ~95%, except for sample AD75 whose efficiency was ~65% and the hypothetic cause is the additional polymerization during the charging process at 0.5 mA.

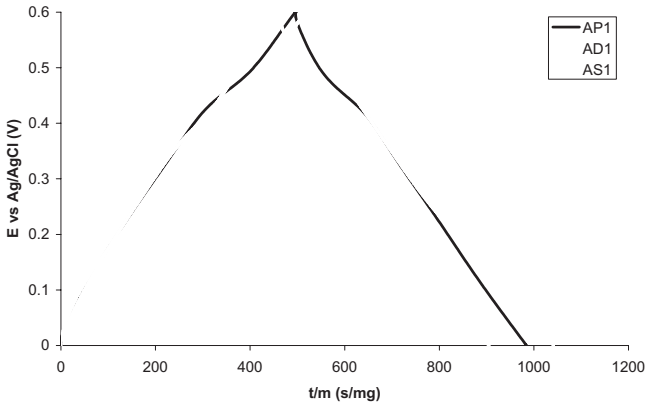

Figure 3. Charge–discharge cycles at 0.5 mA. 1 M HCl + 0.5 M KCl solution. Polymerization methods at 1 V.

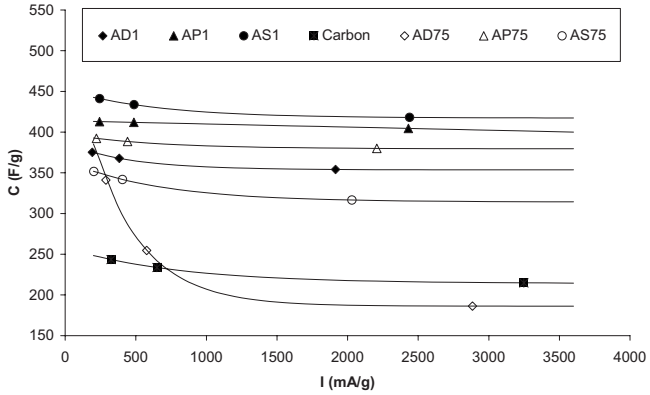

Figure 4. Capacitance values determined by chronopotentiometry vs current.

The capacitance values as a function of the applied current for all the activated carbon/polyaniline composites and the pristine activated carbon are compared in Fig. 4. It can be observed that samples prepared at higher potentials (closed symbols) present higher capacitance, and in all cases, the values are higher than that of the pristine activated carbon. Table III shows the loss of capacitance for each sample when the applied current was increased from 200 to 3000 mA/g.

It can be observed that in all cases, except for sample AD75, the capacitance loss is lower for the composites than for the pristine activated carbon. For samples prepared by the same method, this loss is lower in composites prepared at the higher potential. The comparison of different polymerization methods indicates that the composites prepared using the potentiostatic method shows a better performance at higher charge/discharge currents. The behavior at high power is thought to be related with the porosity of the material, that is, the easiness for the charge balancing ions to reach the available surface area. In potentiodynamic polymerization, the growth of the polymer is periodically interrupted and the deposited polymer chains have time to rearrange themselves to occupy less space. Therefore, the polymer film should be more homogeneous and compact.[20] However, for potentiostatic polymerization, the polymer growth was continuous and fast, which favors the development of a more porous film. Different morphologies of polyaniline electrochemically grown on different electrodes were obtained by different authors,[33-36] and in general, the majority of authors admit that the characteristics of the polymer depend on the mode of synthesis.[34] In agreement with this understanding, composites prepared by the multistep potentiostatic polymerization presented an intermediate behavior. Unfortunately, scanning electron microscopy (SEM) obser-

Table III. Capacitance loss and resistance for each composite.

Sample	Capacitance loss (%)	Resistance (Ω)
A	13	23
AP1	3	14
AP75	3	11
AD1	6	15
AD75	52	26
AS1	6	11
AS75	11	15

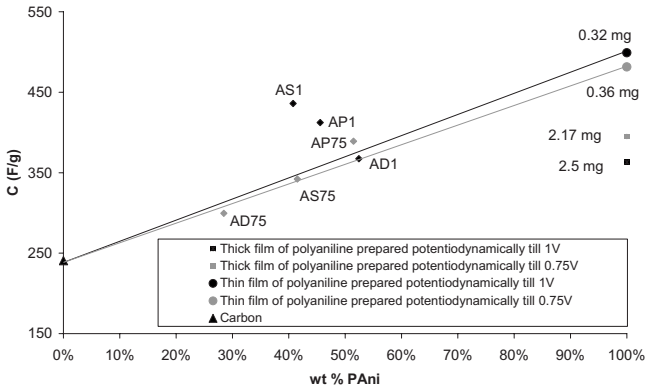

Figure 5. Capacitance values of the composites vs the polyaniline content.

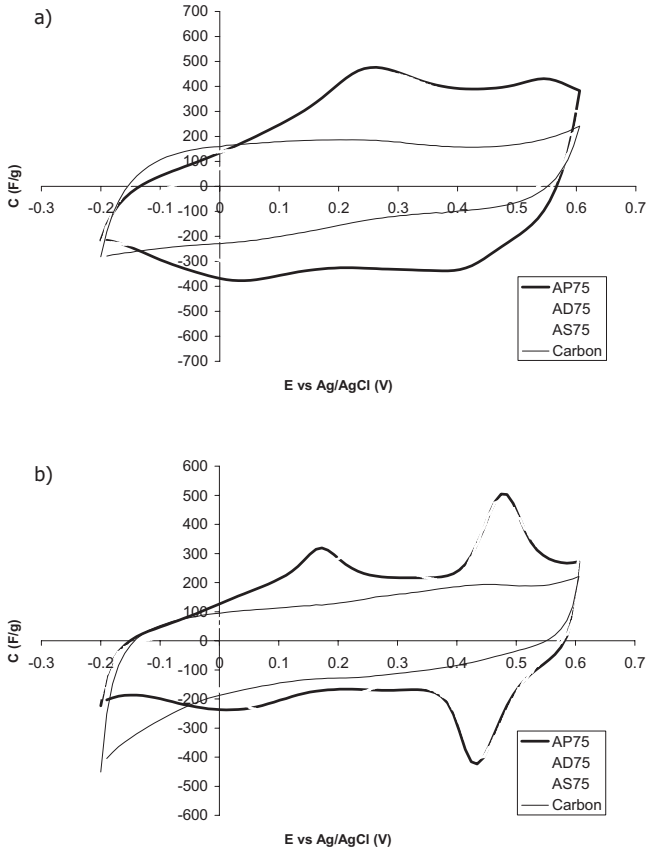

Figure 6. Steady-state voltammograms obtained for the composite samples obtained with the polymerization methods at 0.75 V, 1.0 M HCl + 0.5 M KCl solution: (a) υ = 10 mV s^{-1} and (b) υ = 1 mV s^{-1}.

vations of the composites did not give any information on the polyaniline morphology because the images from the activated carbon did not have any difference with the composites. This is in agreement with the growth of polyaniline inside the porosity of the porous carbon. All these observations suggest that the faster the polymerization is, the higher the porosity in the films is. Consequently, samples prepared potentiostatically at lower potentials or by the potentiodynamic method, that is at a lower polymerization rate, present more compact morphology, which is not favored for high charge/discharge rates. However, it must be pointed out that if the applied potential is too high, overoxidation of the polymer can occur during the polymerization process, which can also lead to inferior capacitive performance.

Figure 5 plots the capacitance of each composite measured at 400 mA/g (interpolating from Fig. 4) against the mass percentage of polyaniline in the composite. For comparison purposes, the results from the pristine activated carbon and some pure polyaniline films are included. The polyaniline films were prepared using the potentiodynamic method because it is well known that such obtained polyaniline is more uniform and adherent to the electrode.[20] It can be seen that, as a general trend, the composites present similar or greater capacitance in comparison to the sum of the individual components in the composite, using the simple mixing rule of each component contributing proportionally. Moreover, it is interesting to remark that this comparison is done with a very thin film of polyaniline of high quality and low mass (0.32 and 0.36 mg). Because the total weight of the composites is ~2 mg, if we compare the results to polyaniline films of similar weight [2.17 and 2.5 mg as indicated in Fig. 5 (see dashed line)] we observe that all the composites present significantly better performance. As has been pointed out before,[26] a cooperative effect of the π-conjugated system of the polymer and the porous carbon material can give larger specific capacitance than just the porous system or the conducting polymer alone. Additionally, an influence of the polyaniline morphology induced by the porous carbon cannot be discarded. The remarkable performance of samples AP1 and AS1 can be due to the contribution of the benzoquinone-hydroquinone redox couple formed upon oxidation at the higher potentials (see next section), which seem to be favored when the polymerization is done in the presence of the activated carbon.

The charge–discharge experiments can also give information about the resistance of the composite. From the ohmic drop of the chronopotentiograms, the resistances have been calculated and are shown in Table III. It can be seen that, as a general trend, the resistance of the composite decreases in relation to the pristine activated carbon; that is to say, the conducting polymer improves the conductivity of the pristine material. From Table III and Fig. 5, it is clear that the composite with the lowest amount of polyaniline shows the highest resistance (sample AD75).

Characterization by cyclic voltammetry.— Figures 6 and 7 present the cyclic voltammograms recorded at 1 and 10 mV s^{-1} of the composites compared to that of the activated carbon. The activated carbon presents a quasi-rectangular shape for both scan rates, indicating that the main contribution to the capacitance is the charge and discharge of the double layer. However, the composites present several overlapped peaks being more defined at lower scan rate, indicating the contribution of redox processes produced by the polyaniline. Moreover, the cyclic voltammogram of the composites compared to that of the activated carbon shows a decrease in the current at lower potentials, where essentially the contribution of the double layer occurs. This suggests that the polymer growth occurred inside of the pores of the activated carbon. It should be noted that SEM observation of the activated carbon and the composites are very similar, in agreement with the above comment. Accordingly, the voltammograms at 1 mV s^{-1} show better defined redox processes of polyaniline because mass transfer is favored at this scan rate. Comparing Fig. 6 and 7, it is interesting to note that the cyclic voltammograms at 10 mV s^{-1} for the composites made by polymerization at 0.75 V present less pronounced peaks than that at 1.0 V. That is, the response of the composites prepared at lower potentials is more capacitive in behavior at 10 mV s^{-1}. Comparing different methods, it can be observed that the potentiodynamically prepared composites present more rectangular voltammograms and hence lower film resistance. However, the total area in the voltammograms is larger and, hence, the capacitance is higher for the potentiostatically made composites.

Regarding the voltammetric peaks, an anodic one between 0.20 and 0.30 V, related to the oxidation of the leucoemeraldine state to emeraldine state of polyaniline, can be distinguished as well as a second peak between 0.50 and 0.60 V (and between 0.40 to 0.50 V

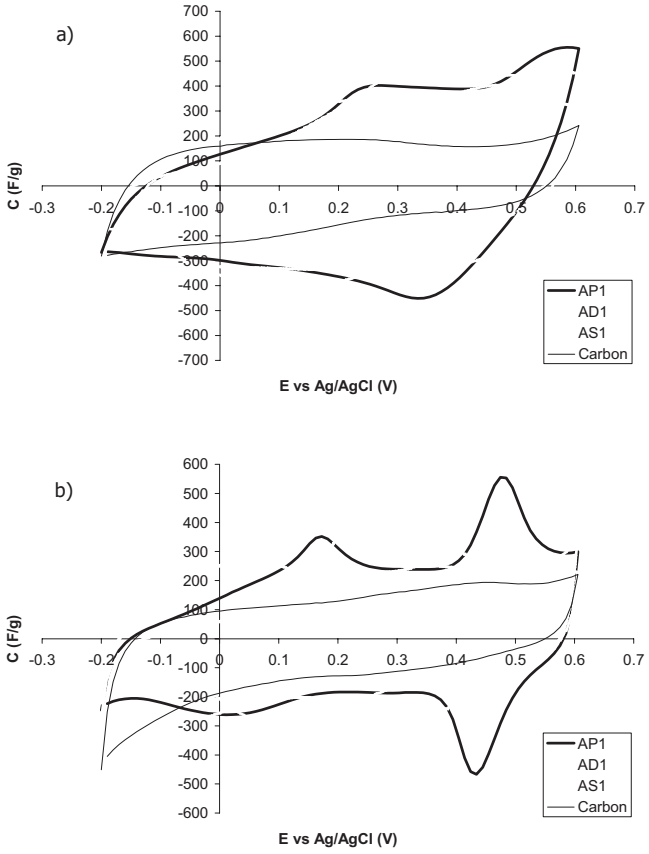

Figure 7. Steady-state voltammograms obtained for the composite samples obtained with the polymerization methods at 1.0 V, 1 M HCl + 0.5 M KCl solution: (a) υ = 10 mV s^{-1} and (b) υ = 1 mV s^{-1}.

at lower scan rate), associated to the benzoquinone-hydroquinone redox couple.[37] The latter process appears when the polyaniline is oxidized at potentials higher than 0.70 V vs saturated calomel electrode in acidic solutions,[38] and it is known to be produced by the degradation products of polyaniline. This process shortens the polymer chains, leaving a more resistive skeleton in the polymer.[38] When degradation takes place, the polyaniline produced has poorer quality because its conductivity decreases. However, when preparing the carbon/polyaniline composites for charge storage, it is important to look for a compromise between capacitance and resistance. The polyaniline degradation produces shorter chains (lower conductivity) but, at the same time, generates benzoquinone groups in the material, which are positive to enhance capacitance by provision of extra faradaic current.[8,9] Then, depending on the application and the required features, different electrochemical methods should be used to prepare the polymer.

Characterization by electrochemical impedance spectroscopy.— Electrochemical impedance spectroscopy provides information about the capacitive and resistive behavior of the samples studied, depending on the frequency, that is to say, the rate of the process. This technique has been used in this study at frequencies from 10 to 4 mHz and a bias potential of 0.30 V. As an example of the results obtained, the corresponding Nyquist plots for the composites prepared potentiostatically are shown in Fig. 8 and 9. The rest of the samples present similar behavior. In Fig. 8 and 9, the corresponding plots for the pristine carbon before the polymerization and a pure polyaniline film prepared under the same conditions are also included for comparison.

The resistive behavior of the samples can be assessed, taking into account the real part of the impedance (insets of Fig. 8 and 9). In this sense, it can be concluded that the pure polyaniline presents

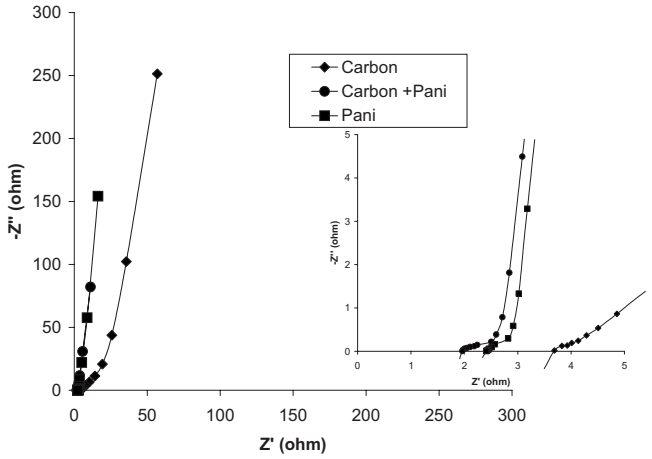

Figure 8. Nyquist plot obtained at 0.30 V for the composites prepared by potentiostatic step at 0.75 V, Q = 2 C. The pristine carbon and a pure polyaniline film are also included, 1 M HCl + 0.5 M KCl solution.

better conductivity than the pristine carbon material and that the composite improves this feature, presenting a lower resistance than the carbon material and very close to the behavior of pure polyaniline.

Regarding the capacitive performance, the capacitance value is usually calculated from the lower frequency values of the imaginary impedance, Z'', according to $Z'' = -(1/2\pi fC)$. Table IV shows the specific capacitance for the pristine activated carbon, pure polyaniline, and the composites obtained by the potentiostatic method at 0.75 and 1.0 V. In addition, the theoretical capacitance of the composite using the mixing rule has been included.

It can be seen that the capacitance of the composite is higher than the theoretical capacitance. Combining with the analysis of the chronopotentiometric data, Table IV suggests a synergic or cooperative effect between the activated carbon and polyaniline on the capacitance of the composite.

Characterization by infrared spectroscopy.— The infrared spectra have been obtained for all the composites prepared and the polyaniline films grown on the bare graphite by the same methods. As explained in the Experimental section, the spectra were acquired in the ATR mode and are presented in Fig. 10.

Polyaniline shows five characteristic absorption bands at 1592, 1497, 1302, 1165, and 828 cm^{-1} (see, as an example, the FTIR

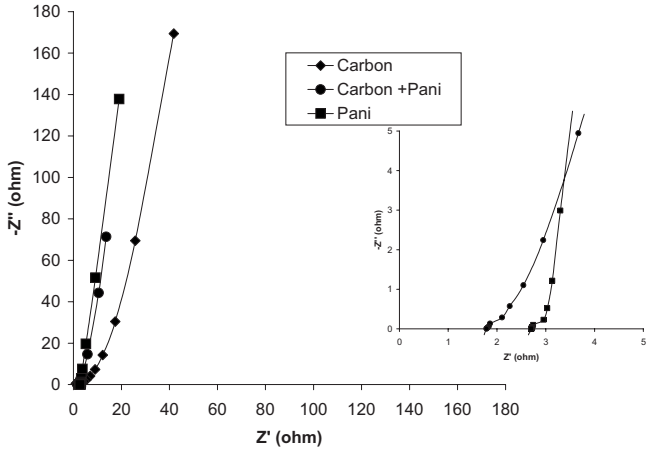

Figure 9. Nyquist plot obtained at 0.3 V for the composite prepared by potentiostatic step at 1 V, Q = 2 C. The pristine activated carbon and a pure polyaniline film are also included, 1 M HCl + 0.5 M KCl solution.

Table IV. Capacitance obtained by electrochemical impedance spectroscopy.

Polymerization potential (V)	Carbon capacitance (F/g)	Polyaniline capacitance (F/g)	Composite capacitance (F/g)	Theoretical capacitance (F/g)	Percent Improvement (%)
0.75	250	100	173	149	16
1.0	250	155	200	186	7

spectrum for sample D1, which is pure polyaniline potentiodynamically grown on graphite at 1.0 V). The band at 1497 cm^{-1} corresponds to the stretching of C = C in benzenoid units related to the reduced state of the polymer, while the band at 1592 cm^{-1} corresponds to the C = N stretching of the quinonimine units produced when polyaniline is oxidized.[39] The band at 1302 cm^{-1} can be associated to the C–H stretching vibration. The bands at 1165 and 828 cm^{-1} belong to the in- and out-plane aromatic C–H bending, respectively.[39-41] Particularly, the band at 1165 cm^{-1} is a an indicator of the degree of electron delocalization along the polyaniline chain.[42] Additionally, an increase in the intensity of the band at 828 cm^{-1} suggests an increase in the 1,4-para-disubstitution character. These bands suggest that the linear structure predominates over the branched one.[41] Table V includes the relative intensities of the 1592, 1165, and 828 cm^{-1} bands obtained in each spectrum related to the 1497 cm^{-1} band (the benzenoid ring) of the polyaniline films grown on the graphite electrode by different methods used in this study.

It can be observed that the faster the polymerization process is (higher potentials), the smaller the relative intensities of the bands at 1165 and 828 cm^{-1} are. As expected, when the polymerization rate is large, the polyaniline obtained is of worse quality: the electron delocalization is lower and the branching of the polyaniline is larger. Both factors can lead to less conducting polymers.

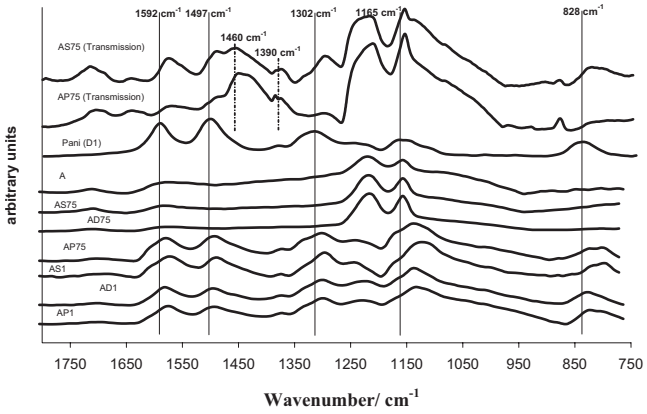

Figure 10. FTIR spectra for all composites, one polyaniline film (D1, potentiodynamically polymerized untill 1 V) and the pristine activated carbon (A), in ATR mode. Additionally, samples AD75 and AS75 are shown in transmission mode.

Table V. Relative intensities of the different bands related to the benzenoid band (1497 cm^{-1}) obtained in each spectrum of polyaniline films grown on the graphite electrode without activated carbon.

Polyaniline film	Relative intensities		
	Band at 1592 cm^{-1}	Band at 1165 cm^{-1}	Band at 828 cm^{-1}
P1	0.72	0.51	0.41
D1	0.81	0.44	0.40
S1	0.74	0.60	0.39
P75	0.85	0.86	0.50
S75	1.04	0.87	0.78

Figure 10 shows the ATR-FTIR spectra for the composites, the pristine carbon material and one of the pure polyaniline films for comparison purposes. It is difficult to observe differences between the composites because of the presence of the carbon material affecting the spectra. However, a shift toward lower wavenumbers, with respect to the bands in pure polyaniline, can be found.

It is also important to note that samples AD75 and AS75 present a completely different ATR-FTIR spectrum from the rest of the composites. The spectra for these samples (AD75 and AS75) are similar to that of the pristine activated carbon, with the bands at 1160 and 1230 cm^{-1} corresponding to PTFE (binder). However, the electrochemical analysis has confirmed the presence of polyaniline in these composites. Thus, the IR spectra of these samples were also obtained in transmission mode (diluting the sample with KBr) [see spectra called AS75 (Transmission) and AD75 (Transmission) in Fig. 10]. Now, the bands corresponding to polyaniline can be observed, although again shifted toward lower wavenumbers with respect to the bands in the pure polymer film. Moreover, additional bands can be observed in these transmission spectra at 1460 and 1390 cm^{-1}, associated to the formation of imines and C–N bonds with intermediate order, which are characteristic of the conducting form of polyaniline and related materials.[43] Thus, it can be concluded that, in these composites (prepared with the slowest polymerization methods), the polymer is located in the inner parts of the porous structure, which is an interesting difference from other composites and possibly a consequence of the lower polymerization rate. Furthermore, the shift of the IR bands to lower wavenumbers corroborates that an interaction exists between the polyaniline and the carbon surface, and it could be indicative of enhanced conjugation along the polyaniline chains.

Conclusions

Carbon/polyaniline composites have been prepared by different electrochemical methods in order to study the electrochemical properties of these composites particularly for supercapacitor applications. In all the tested methods, the amount of polyaniline is higher on the activated carbon electrode than on the bare graphite electrode. This effect is attributed to the greater surface area of the porous activated carbon. It has been shown that the capacitance of the as-prepared composites is larger than the simple addition of the capacitance measured from the individual components alone. This finding demonstrated that the electrochemical combination of these two materials into a properly structured composite can synergistically or cooperatively lead to enhanced capacitance. This synergistic effect is believed to have resulted from at least three factors. First, the dispersed deposition of a thin polyaniline film onto the large external and internal surfaces of the porous activated carbon is beneficial to increasing the charge transfer kinetics and more completely utilizing the polymer. Second, as confirmed by FTIR analyses, the activated carbon is capable of enhancing the electron delocalization along the polyaniline chains in the composite, which increases the intrinsic charge storage capacity of the polymers. Moreover, the resistance of the composite is lower than that of the pristine carbon material, indicating the beneficial effect of the polymer in provision of additional electron pathways.

It has been observed that the single-step potentiostatic methods are able to produce composites with larger capacitance and better performances in the high-power regime. The potentiodynamically prepared composites possess higher conductivities, likely because of

the polyaniline being in a more compact and uniform structure. Composite samples prepared by the multistep potentiostatic methods perform intermediately between the single-step potentiostatic and the potentiodynamic methods. It becomes evident from the findings of this work that careful selection and application of one of the various electrochemical polymerization methods is needed, depending on the requirements of specific applications of the composite.

Acknowledgments

The authors are grateful to MEC for financial support (project no. CTQ2006-08958/PPQ and no. MAT2006-60621) and Generalitat Valenciana-Feder (FTIR Microscopy equipment). M.J.B.-M. thanks MEC for the thesis grant and K. C. Ng for support in the laboratory of Nottingham University.

University of Alicante assisted in meeting the publication cost of this artile.

References

1. B. E. Conway, *Electrochemical Supercapacitors: Scientific Fundamentals and Technological Applications*, Kluwer Academic/Plenum Publishers, New York, (1999).
2. E. Raymundo-Piñero, V. Khomenko, E. Frackoviak, and F. Béguin, *J. Electrochem. Soc.*, **152**, A229 (2005).
3. O. Barbieri, M. Hahn, A. Foelske, and R. Kotz, *J. Electrochem. Soc.*, **153**, A2049 (2006).
4. C. C. Hu, W. C. Chen, and K. H. Chang, *J. Electrochem. Soc.*, **151**, A281 (2004).
5. I. H. Kim and K. B. Kim, *J. Electrochem. Soc.*, **153**, A383 (2006).
6. J. Chmiola, G. Yushin, Y. Gogotsi, C. Portes, P. Simon, and P. L. Taberna, *Science*, **313**, 1760 (2006).
7. E. Raymundo-Piñero, K. Kierzek, J. Machnikowski, and F. Béguin, *Carbon*, **44**, 2498 (2006).
8. M. J. Bleda-Martinez, J. A. Macia-Agullo, D. Lozano-Castello, E. Morallon, D. Cazorla-Amoros, and A. Linares-Solano, *Carbon*, **43**, 2677 (2005).
9. M. J. Bleda-Martinez, D. Lozano-Castello, E. Morallon, D. Cazorla-Amoros, and A. Linares-Solano, *Carbon*, **44**, 2642 (2006).
10. D. Lozano-Castello, D. Cazorla-Amoros, A. Linares-Solano, S. Shiraishi, H. Kurihara, and A. Oya, *Carbon*, **41**, 1765 (2003).
11. K. Jurewicz, K. Babal, A. Ziolkowski, and H. Wachowska, *Electrochim. Acta*, **48**, 1491 (2003).
12. D. Hulicova, J. Yamashita, Y. Soneda, H. Hatori, and M. Kodama, *Chem. Mater.*, **17**, 1241 (2005).
13. V. Gupta and N. Miura, *Electrochem. Solid-State Lett.*, **8**, A630 (2005).
14. C. C. Hu and J. Y. Lin, *Electrochim. Acta*, **47**, 4055 (2002).
15. J. M. Ko, R. Song, H. J. Yu, J. W. Yoon, B. G. Min, and D. W. Kim, *Electrochim. Acta*, **50**, 873 (2004).
16. K. S. Ryu, K. M. Kim, N. G. Park, Y. J. Park, and S. H. Chang, *J. Power Sources*, **103**, 305 (2002).
17. K. R. Prasad and N. J. Munichandraiah, *J. Electrochem. Soc.*, **149**, A1393 (2002).
18. H. H. Zhou, H. Chen, S. L. Luo, G. W. Lu, W. Z. Wei, and Y. F. J. Kuang, *J. Solid State Electrochem.*, **9**, 574 (2005).
19. F. Fusalba, P. Gouerec, D. Villers, and D. Belanger, *J. Electrochem. Soc.*, **148**, A1 (2001).
20. S. K. Mondal, K. R. Prasad, and N. Munichandraiah, *Synthesis*, **148**, 275 (2005).
21. W. C. Chen, T. C. Wen, and H. S. Teng, *Electrochim. Acta*, **48**, 641 (2003).
22. C. Dalmolin, S. C. Canobre, S. R. Biaggio, R. C. Rocha-Filho, and N. Bocchi, *J. Electroanal. Chem.*, **578**, 9 (2005).
23. C. C. Hu, W. Y. Li, and J. Y. Lin, *J. Power Sources*, **137**, 152 (2004).
24. Y. R. Lin and H. S. Teng, *Carbon*, **41**, 2865 (2003).
25. S. K. Mondal, K. Barai, and N. Munichandraiah, *Electrochim. Acta*, **52**, 3258 (2007).
26. H. Talbi, P. E. Just, and L. H. Dao, *J. Appl. Electrochem.*, **33**, 465 (2003).
27. M. Q. Wu, G. A. Snook, V. Gupta, M. Shaffer, D. J. Fray, and G. Z. Chen, *J. Mater. Chem.*, **15**, 2297 (2005).
28. M. J. Bleda-Martinez, E. Morallon, and D. Cazorla-Amoros, *Electrochim. Acta*, **52**, 4962 (2007).
29. V. Khomenko, E. Frackowiak, and F. Béguin, *Electrochim. Acta*, **50**, 2499 (2005).
30. D. Lozano-Castello, M. A. Lillo-Rodenas, D. Cazorla-Amoros, and A. Linares-Solano, *Carbon*, **39**, 741 (2001).
31. D. Cazorla-Amoros, J. Alcaniz-Monge, M. A. Casa-Lillo, and A. Linares-Solano, *Langmuir*, **14**, 4589 (1998).
32. Z. Mandic, L. Duic, and F. Kovacicek, *Electrochim. Acta*, **42**, 1389 (1997).
33. W. Huang, B. D. Humphrey, and A. G. MacDiarmid, *J. Chem. Soc., Faraday Trans.*, **1**, 2385 (1986).
34. E. M. Genies, A. Boyle, M. Lapkowski, and C. Tsintavis, *Synth. Met.*, **36**, 139 (1990).
35. A. Kitani, J. Yano, and K. Sasaki, *Chem. Lett.*, **9**, 1565 (1984).
36. A. F. Díaz and J. A. Logan, *J. Electroanal. Chem. Interfacial Electrochem.*, **111**, 111 (1980).
37. E. I. Santiago, E. C. Pereira, and L. O. S. Bulhoes, *Synth. Met.*, **98**, 87 (1998).
38. K. Aoki and S. Tano, *Electrochim. Acta*, **50**, 1491 (2005).
39. G. Socrates, *Infrared and Raman Characteristics Frequencies of Organic Molecules*, John Wiley & Sons, Hoboken, NJ, (2001).
40. R. Singh, V. Arora, R. P. Tandon, S. Chandra, N. Kumar, and A. Mansingh, *Polymer*, **38**, 4897 (1997).
41. C. M. Yang, C. Y. Chen, and Y. Zeng, *Spectrochim. Acta, Part A*, **66**, 37 (2007).
42. J. C. Chiang and A. G. Macdiarmid, *Synth. Met.*, **13**, 193 (1986).
43. M. A. Cotarelo, F. Huerta, R. Mallavia, E. Morallon, and J. L. Vazquez, *Synth. Met.*, **156**, 51 (2006).

AUTHOR QUERIES — 011810JES

#1 Author-line 13, Please check inserted definition for ″FTIR″ in abstract
#2 Author, line 96, Please check definition for ″BET″ in /of paragraph of Experimental Section. was this your content?
#3 Author, line 107, Please define ″PTFE″ at first use. see ″Electrodes fabrication″ section.
#4 Author, lines 150 & 151, please check difinition of ″MCT″ and ″ATR″
#5 Author, line 339, please check ″SCE,″ defined as ″saturated colonel electrode″ was this you intent?